Thermochimica Acta, 230 (1993) 1–13
Elsevier Science Publishers B.V., Amsterdam
SSDI 0040-6031(93)01185-6

Calculations of excess enthalpies of binary systems at high pressures by means of a cubic equation of state

Tatsuhiko Ohta

Department of Chemistry and Chemical Engineering, Division of Physical Sciences, Kanazawa University, Kodatsuno 2-40-20, Kanazawa, Ishikawa 920 (Japan)

(Received 3 March 1993; accepted 26 March 1993)

Abstract

The molar excess enthalpies H^E of various kinds of binary systems at high pressures are represented by the PRSV equation of state coupled with the NRTL mixing rule. 47 sets of data for binary H^E in the liquid, two-phase, and gaseous regions are studied. Good agreement is obtained between calculated and experimental values for all the systems.

LIST OF SYMBOLS

a	parameter of the equation of state
a_{ij}	binary interaction parameter
A	amount of phase I
b	parameter of the equation of state
B	amount of phase II
c	numerical constant, equal to $2\sqrt{2}/\ln[(2+\sqrt{2})/(2-\sqrt{2})]$
C_{ij}, D_{ij}	coefficients of eqn. (17)
G_{ij}	coefficient defined by eqn. (15)
G^E_∞	excess Gibbs energy at infinite pressure
H^E	excess enthalpy
$\Delta H'$	enthalpy departure function
P	total pressure
R	gas constant
T	absolute temperature
v	molar volume
x	mole fraction
z	compressibility factor

Greek letters

α	function of reduced temperature and acentric factor
α_{ij}	non-randomness parameter

τ	binary parameter
ω	acentric factor
κ	function of reduced temperature and acentric factor
κ_0	function of acentric factor
κ_1	pure component parameter

Subscripts

c	critical property
i, j	components
M	actual composition of mixture
R	reduced temperature
I, II	phases I and II
∞	at infinite pressure

Superscript

E	excess property

INTRODUCTION

Recently, the flow calorimeter has become well established for the determination of excess enthalpy (H^E) data at elevated temperatures and pressures. As a result of its development, the H^E data in the critical region are available for the testing of thermodynamic models. There have been several reports discussing the representation of binary H^E data in the high pressure region by the use of equations of state [1–6].

The PRSV equation of state [7,8] is useful in the representation of thermodynamic properties. The calculations of vapor–liquid equilibria (VLE) have been successfully made for binary and multicomponent systems at low pressures using the equation of state with the Huron–Vidal mixing rules [9]. Furthermore, this equation of state has been extended to predict ternary excess enthalpy data from binary H^E data alone for highly non-ideal systems at ambient pressure [10].

It is the purpose of this work to show that the PRSV equation of state with the NRTL mixing rule is capable of representing the excess enthalpies in the liquid, two-phase, and gaseous regions for various kinds of binary mixtures containing non-polar, polar, and associating substances.

CALCULATION OF EXCESS ENTHALPY

Lewis et al. [1] have presented the derivation of excess enthalpies from an equation of state. The excess enthalpy H^E is calculated in terms of the enthalpy departures as

$$H^E = \Delta H' - \sum_i x_i \Delta H_i' \qquad (1)$$

where x_i is the mole fraction of component i, and $\Delta H_i'$ and $\Delta H'$ are the enthalpy departure functions for pure components and mixtures. These functions can be obtained from an equation of state using the thermodynamic relation

$$\Delta H' = \int_{\infty}^{v} [T(\partial P/\partial T)_v - P]\,\mathrm{d}v + RT(z-1) \qquad (2)$$

where $z = Pv/RT$.

The enthalpy calculations for the mixture in the two-phase region were made on the following basis. A mixture consists of amounts A of phase I and B of phase II. The compositions of phases I and II in equilibrium are x_{I} and x_{II} respectively. When the actual composition of the mixture is given by x_{M} the equations

$$x_{\mathrm{I}}A + x_{\mathrm{II}}B = x_{\mathrm{M}} \qquad (3)$$

$$(1 - x_{\mathrm{I}})A + (1 - x_{\mathrm{II}})B = 1 - x_{\mathrm{M}} \qquad (4)$$

must be satisfied where x_{M}, x_{I} and x_{II} are mole fractions of the same component. When we solve for A and B, the enthalpy departure of the mixture is given by

$$\Delta H' = A(\Delta H_{\mathrm{M}}')_{\mathrm{I}} + B(\Delta H_{\mathrm{M}}')_{\mathrm{II}} \qquad (5)$$

where $(\Delta H_{\mathrm{M}}')_{\mathrm{I}}$ and $(\Delta H_{\mathrm{M}}')_{\mathrm{II}}$ are the enthalpy departure functions of phase I of composition x_{I} and phase II of composition x_{II}.

THE PRSV EQUATION OF STATE WITH THE NRTL MIXING RULE

In this work the PRSV equation of state is selected to evaluate the $\Delta H'$. It has the cubic in volume form of the Peng–Robinson equation of state [11]

$$P = \frac{RT}{v-b} - \frac{a}{v(v+b) + b(v-b)} \qquad (6)$$

with

$$a = (0.457235R^2T_{\mathrm{c}}^2/P_{\mathrm{c}})\alpha \qquad (7)$$

$$b = 0.077796RT_{\mathrm{c}}/P_{\mathrm{c}} \qquad (8)$$

where

$$\alpha = [1 + \kappa(1 - T_{\mathrm{R}}^{0.5})]^2 \qquad (9)$$

The expression for the term κ is given by Stryjek and Vera [7, 8].

$$\kappa = \kappa_0 + \kappa_1(1 + T_{\mathrm{R}}^{0.5})(0.7 - T_{\mathrm{R}}) \qquad (10)$$

where

$$\kappa_0 = 0.378893 + 1.4897153\omega - 0.17131848\omega^2 + 0.0196554\omega^3 \qquad (11)$$

and κ_1 is a pure component adjustable parameter, which is available in the literature [8, 12], together with critical constants and the acentric factor.

For mixtures, the NRTL mixing rule developed by Huron and Vidal [13] was utilized, i.e.

$$a = b\left(\sum_i x_i \frac{a_{ii}}{b_i} - cG^{\mathrm{E}}_{\infty}\right) \tag{12}$$

$$b = \sum_i x_i b_i \tag{13}$$

where c is the numerical constant which depends on the equation of state. The NRTL equation [14] was employed to represent the excess Gibbs free energy at infinite pressure G^{E}_{∞}, i.e.

$$G^{\mathrm{E}}_{\infty}/RT = \sum_i x_i \frac{\sum_j \tau_{ji} G_{ji} x_j}{\sum_k G_{ki} x_k} \tag{14}$$

with

$$G_{ij} = \exp(-\alpha_{ij}\tau_{ij}) \tag{15}$$

$$\tau_{ij} = a_{ij}/T \tag{16}$$

where α_{ij} $(= \alpha_{ji})$ is a non-randomness constant. The values of α_{ij} for binary systems were taken from previous papers [9, 10]. The binary energy parameters a_{ij} were assumed to change linearly with temperature, i.e.

$$a_{ij} = C_{ij} + D_{ij}(T - 273.15) \tag{17}$$

The adjustable parameters C_{ij} and D_{ij} were determined by the simplex method [15], which minimizes the sum of the squares of deviations in experimental and calculated H^{E} values.

RESULTS

It is convenient to classify the calculated results into three groups: the results in the liquid region, in the vicinity of the critical region, and in the gaseous region.

The liquid region

Fifteen sets of binary data for strongly non-ideal liquid systems were studied, and the calculated results are listed in Table 1.

Of the *n*-butane–alcohol mixtures at 298.15 K and 2.985 MPa, three representative examples are shown in Fig. 1.

TABLE 1

Calculated results for binary systems in the liquid region

System (1–2)	Temperature in K	Pressure in MPa	No. of data points	Parameter					Abs. arith. mean dev.		Ref.
				C_{12} in K	D_{12}	C_{21} in K	D_{21}	α_{12}	δH^E in J mol^{-1}	$\delta H^E/H^E$ in %	
n-Butane–methanol	298.15	2.985	23	2725.84	12.2513	466.51	0.8033	0.41	4.1	1.3	16
n-Butane–ethanol	298.15	2.985	28	1669.38	4.0823	−208.42	−1.7161	0.41	7.7	4.2	16
n-Butane–*n*-propanol	298.15	2.985	30	1945.28	4.7999	−633.93	−3.3680	0.41	3.1	1.7	16
n-Butane–*n*-butanol	298.15	2.985	33	2167.65	4.0992	−730.31	−3.8284	0.41	3.2	2.5	16
n-Butane–*n*-pentanol	298.15	2.985	29	2131.45	5.0864	−767.82	−3.8326	0.41	6.3	3.0	16
n-Butane–*n*-hexanol	298.15	2.985	30	1996.32	4.4093	−694.72	−3.5536	0.41	5.8	4.1	16
n-Butane–*n*-octanol	298.15	2.985	23	1812.93	4.2150	−566.44	−2.9226	0.41	2.2	1.0	16
n-Butane–*n*-decanol	298.15	2.985	34	1795.96	3.7916	−419.80	−2.4357	0.41	8.1	5.5	16
1-Butene–methyl *t*-butyl ether	293.15	1.806	13	145.76	0.7721	114.87	0.3597	0.30	0.7	2.0	17
	333.15	1.944	16	−50.98	0.3780	336.47	1.0007	0.30	1.3	22.9	17
Ethanol–water	333.15	0.4	23	430.39	3.0137	857.63	6.9812	0.30	2.6	9.0	18
	423.15	5.0	19	234.91	3.7299	209.89	−1.9295	0.30	4.2	1.3	19
	473.15	5.0	19	153.94	−0.8620	634.83	0.8696	0.30	3.8	0.8	19
Cyclohexane–acetonitrile	323.15	15.0	23	1649.96	1.8682	481.21	−3.1945	0.32	9.2	1.7	20
	348.15	15.0	29	1153.79	0.3976	608.60	−2.2007	0.32	5.6	0.6	20

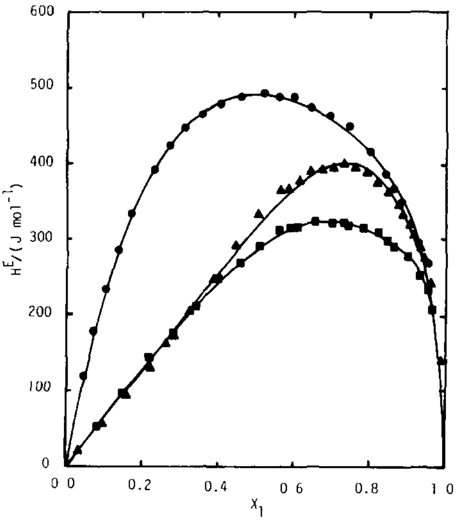

Fig. 1. Comparison of experimental and calculated excess enthalpies for *n*-butane(1)–alcohol(2) systems at 298.15 K and 2.985 MPa. Experimental (McFall et al. [16]): ●, *n*-butane(1)–methanol(2); ▲, *n*-butane(1)–*n*-pentanol(2); ■, *n*-butane(1)–*n*-octanol(2). Calculated: ——.

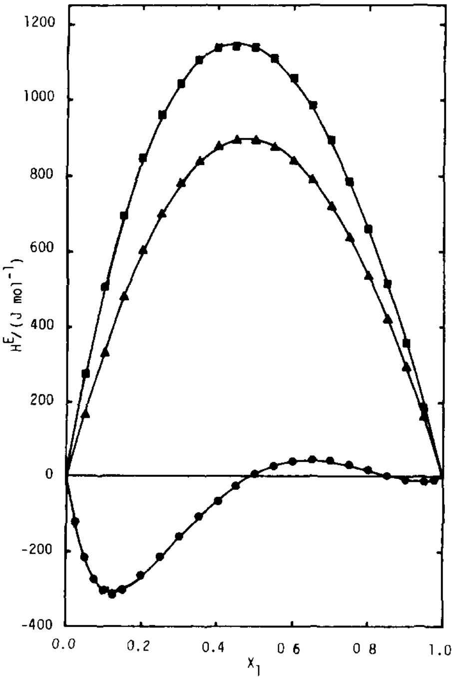

Fig. 2. Comparison of experimental and calculated excess enthalpies for the ethanol(1)–water(2) system. Experimental: ●, at 333.15 K and 0.4 MPa (Ott et al. [18]); ▲, at 423.15 K and 5.0 MPa (Ott et al. [19]); ■, at 473.15 K and 5.0 MPa (Ott et al. [19]). Calculated: ——.

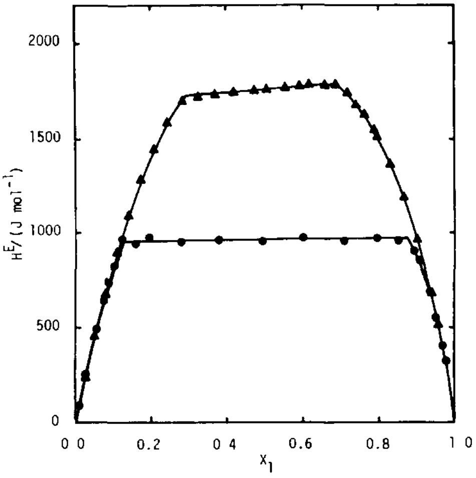

Fig. 3. Comparison of experimental and calculated excess enthalpies for the cyclohexane(1)–acetonitrile(2) system at 15.0 MPa. Experimental (Ott et al. [20]): ●, at 323.15 K; ▲, at 348.15 K. Calculated: ——.

For the ethanol–water system at 333.15 K and 0.4 MPa, which gives rise to a double minimum in H^E, the present equation of state can reproduce the unusual data with good accuracy, as shown in Fig. 2.

Figure 3 shows the results for the partially miscible cyclohexane–acetonitrile system where the H^E vs. x curves have a linear portion due to liquid–liquid phase separation. The calculated results are in excellent agreement with the experimental data.

The vicinity of the critical region

The H^E values in the critical region vary markedly with temperature, pressure, and composition. Twenty-four sets of binary data for three mixtures in the vicinity of the critical region were investigated here. Table 2 shows the results for these mixtures.

Plots of H^E vs. x for the carbon dioxide–cyclohexane system at three temperatures are shown in Fig. 4. The dramatic changes in H^E are caused by phase changes within the critical locus. The linear sections of the isotherm-isobars in Fig. 4 correspond to two-phase regions in which gaseous and liquid phases of fixed composition are in equilibrium. The shapes of the calculated H^E curves are very close to those of the experimental data.

Figure 5 shows the results for the ethane–chlorodifluoromethane (Freon-22) system over the entire composition range at nine temperatures and 5.15 MPa. The curves of H^E vs. x in the two-phase region can be well

TABLE 2

Calculated results for binary systems in the vicinity of the critical region

System (1–2)	Temperature in K	Pressure in MPa	No. of data points	Parameter					Abs. arith. mean dev.		Ref.
				C_{12} in K	D_{12}	C_{21} in K	D_{21}	α_{12}	δH^E in J mol^{-1}	$\delta H^E/H^E$ in %	
Carbon dioxide–cyclohexane	308.15	7.50	29	738.13	0.7862	−317.60	−4.0386	0.40	161.3	20.6	21
		10.50	34	976.26	−1.0657	−3.00	−3.6148	0.40	6.9	3.5	21
		12.50	31	905.36	−0.6137	2.20	−3.3681	0.40	4.4	3.6	21
	358.15	7.50	43	219.06	15.8943	3146.63	11.8008	0.40	22.6	20.2	21
		10.50	41	801.56	4.2443	9.93	−2.5661	0.40	6.4	2.6	21
		12.50	35	739.62	3.7386	12.88	−2.6755	0.40	9.8	30.1	21
	413.15	7.50	58	873.30	8.3746	−369.05	−4.2804	0.40	25.9	5.3	21
		10.50	55	157.14	8.3683	21.19	−1.2015	0.40	19.1	4.7	21
		12.50	41	618.41	2.4872	2.46	−2.1071	0.40	8.4	4.5	21
Ethane–Freon-22	293.15	5.15	26	340.75	0.5824	−94.39	−1.6977	0.30	6.9	3.2	22
	303.15	5.15	28	291.74	−0.2900	6.97	−0.7299	0.30	6.7	5.8	22
	313.15	5.15	33	866.79	15.2914	−427.22	−2.8712	0.30	63.9	14.7	22
	323.15	5.15	33	672.34	17.5237	−356.30	−1.6773	0.30	46.4	7.8	22
	333.15	5.15	30	767.92	13.3620	−295.26	−1.0488	0.30	61.8	26.4	22
	343.15	5.15	33	422.56	33.1013	−357.58	2.8029	0.30	98.7	36.5	22
	363.15	5.15	39	−600.44	25.4322	468.50	−9.1682	0.30	217.5	23.8	22
	373.15	5.15	24	−112.45	−5.9382	1100.95	−1.7682	0.30	38.8	5.5	22
	383.15	5.15	29	−242.02	0.5702	751.52	−5.3540	0.30	16.4	4.4	22
Ethane–methanol	298.15	7.5	31	1187.86	2.6887	−191.76	−1.7378	0.41	7.0	20.4	23
		15.0	23	1468.72	6.0779	−344.47	−1.9504	0.41	12.9	13.2	23
	323.15	7.5	24	1220.68	8.7144	0.18	−0.1866	0.41	7.3	8.6	23
		15.0	29	1464.36	2.8072	−406.39	−2.8922	0.41	9.4	7.2	23
	348.15	7.5	29	2532.82	−7.6651	−108.78	−3.8166	0.41	3.0	1.9	23
		15.0	33	1863.07	−1.6538	−399.16	−4.0978	0.41	10.5	6.8	23

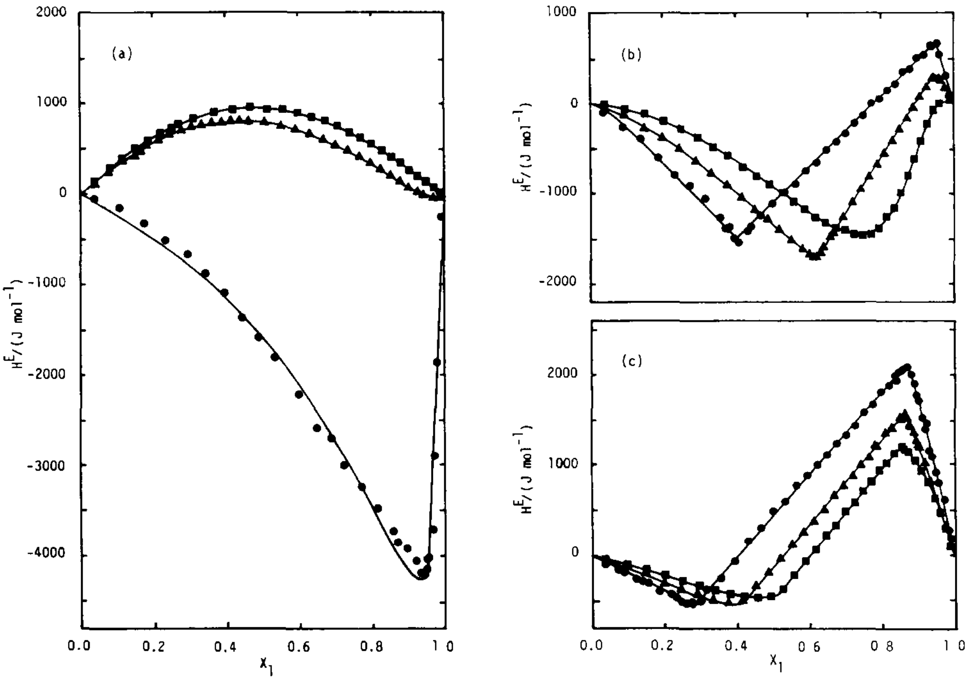

Fig. 4. Comparison of experimental and calculated excess enthalpies for the carbon dioxide(1)-cyclohexane(2) system at 308.15, 358.15, and 413.15 K. Experimental (Christensen et al. [21]): ●, at 7.50 MPa; ▲, at 10.50 MPa; ■, at 12.50 MPa; (a) at 308.15 K; (b) at 358.15 K; (c) at 413.15 K. Calculated: ——.

reproduced from the present equation of state, and in the other liquid and gaseous regions. The deviations of the calculated results from the experimental values for this system are much smaller than those of Christensen et al. [4], who used seven equations of state.

A wide diversity of shapes is obtained for H^E vs. x plots of the ethane-methanol system at 298.15, 323.15, and 348.15 K and at pressures of 7.5 and 15 MPa, as shown in Fig. 6. Figure 6(a) indicates that the equation of state works well for the system where liquid-liquid and vapor-liquid equilibria are present at 298.15 K and at 323.15 and 348.15 K respectively. As shown in Fig. 6(b), however, the results for the system at 15 MPa which forms a supercritical single-phase fluid mixture at each temperature slightly deviate from the experimental data.

The gaseous region

The excess enthalpies of eight sets of binary data for three gaseous mixtures were also calculated using the above equation of state. The results for these mixtures are given in Table 3. Figure 7 illustrates three examples of these. Good representation of the experimental data is obtained.

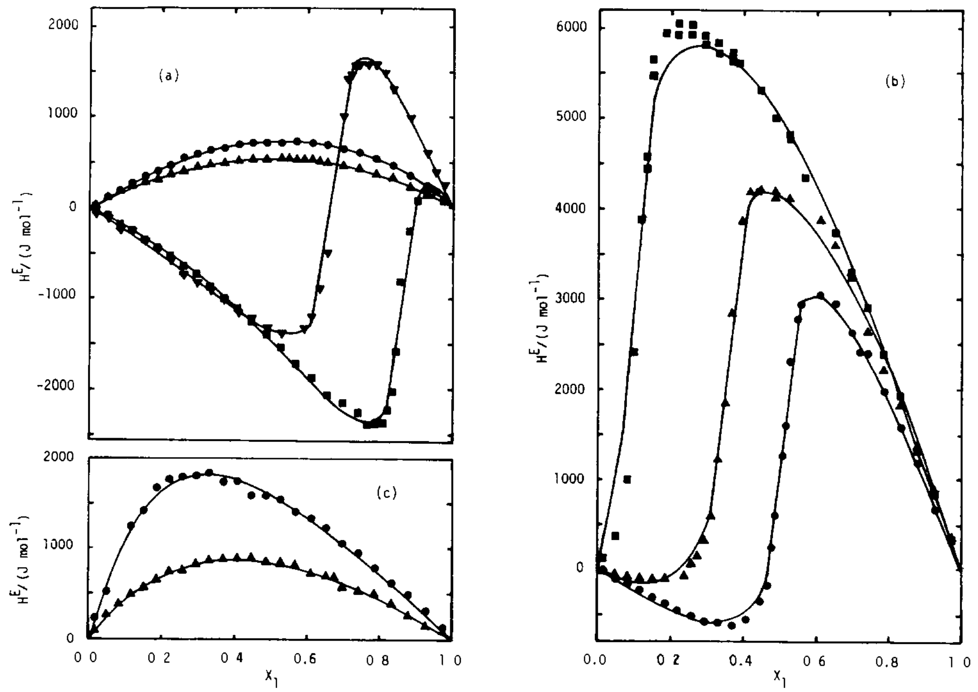

Fig. 5. Comparison of experimental and calculated excess enthalpies for the ethane(1)–Freon-22(2) system at 5.15 MPa. Experimental (Christensen et al. [22]): (a) ●, at 293.15 K; ▲, at 303.15 K; ■, at 313.15 K; ▼, at 323.15 K. (b) ●, at 333.15 K; ▲, at 343.15 K; ■, at 363.15 K. (c) ●, at 373.15 K; ▲, at 383.15 K. Calculated: ——.

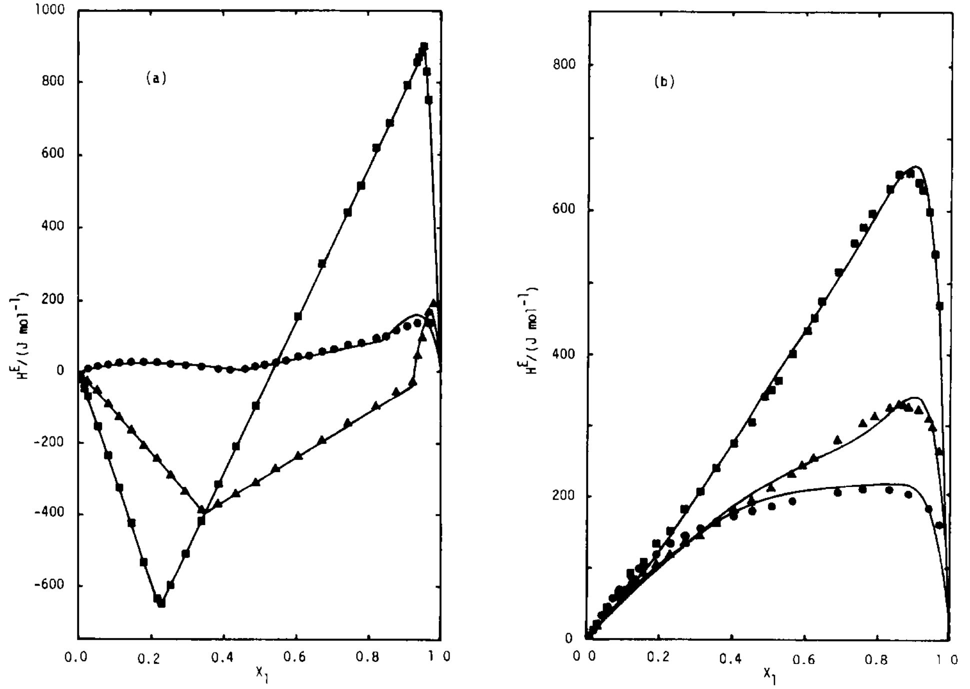

Fig. 6. Comparison of experimental and calculated excess enthalpies for the ethane(1)–methanol(2) system at 7.5 and 15.0 MPa. Experimental (Sipowska et al. [23]): ●, at 298.15 K; ▲, at 323.15 K; ■, at 348.15 K. (a) at 7.5 MPa; (b) at 15.0 MPa. Calculated: ——.

TABLE 3

Calculated results for binary systems in the gaseous region

System (1–2)	Temperature in K	Pressure in MPa	No. of data points	Parameter					Abs. arith. mean dev.		Ref.
				C_{12} in K	D_{12}	C_{21} in K	D_{21}	α_{12}	δH^E in J mol^{-1}	$\delta H^E/H^E$ in %	
Nitrogen–methane	201	5.56	6	−441.71	−2.6967	284.16	−0.7582	0.60	3.8	0.8	24
		7.14	10	436.29	4.2846	−272.07	−3.7508	0.60	21.0	2.4	24
		8.15	4	1153.15	10.7787	88.49	0.4180	0.60	15.6	1.6	24
	298	10.23	5	−29.80	−0.0085	74.03	−0.3083	0.60	0.6	0.5	24
Methane–ethylene	293.15	1.114	4	214.61	−1.1747	−69.83	0.8191	0.30	0.5	2.1	3
	313.15	3.445	4	132.40	−0.0007	194.56	3.6253	0.30	7.8	7.6	3
Methane–carbon dioxide	313.15	1.013	11	228.25	−0.3829	710.01	1.6475	0.40	0.8	2.8	25
		3.546	5	553.33	4.6555	373.92	1.9516	0.40	1.5	1.3	25

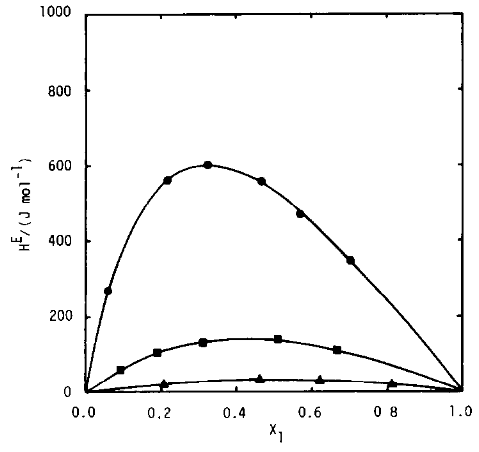

Fig. 7. Comparison of experimental and calculated excess enthalpies for gaseous systems. Experimental: ●, nitrogen(1)–methane(2) at 201 K and 5.56 MPa (Wormald et al. [24]); ▲, methane(1)–ethylene(2) at 293.15 K and 1.114 MPa (Gagne et al. [3]); ■, methane(1)–carbon dioxide(2) at 313.15 K and 3.546 MPa (Barry et al. [25]). Calculated: ——.

CONCLUSIONS

The PRSV equation of state coupled with the NRTL mixing rule were utilized for the calculation of excess enthalpies of strongly non-ideal systems at high pressures including the vicinity of the critical region. The present approach for the binary systems gives good results with sufficient accuracy.

REFERENCES

1 K.L. Lewis, S.E. Mosedale and C.J. Wormald, J. Chem. Thermodyn., 9 (1977) 121.
2 C.J. Wormald, Fluid Phase Equilib., 28 (1986) 137.
3 C. Gagne, S.C. Kaliaguine and R.S. Ramalho, J. Chem. Eng. Data, 31 (1986) 298.
4 J.J. Christensen, R.M. Izatt and D.M. Zebolsky, Fluid Phase Equilib., 38 (1987) 163.
5 J.B. Ott, J. Chem. Thermodyn., 22 (1990) 1129.
6 G. Chen, Z. Wu, Z. Chen and Y. Hou, Fluid Phase Equilib., 65 (1991) 145.
7 R. Stryjek and J.H. Vera, ACS Symp. Ser., 300 (1986) 560.
8 R. Stryjek and J.H. Vera, Can. J. Chem. Eng., 64 (1986) 323.
9 T. Ohta, Thermochim. Acta, 185 (1991) 283.
10 T. Ohta, Thermochim. Acta, 202 (1992) 51.
11 D.Y. Peng and D.B. Robinson, Ind. Eng. Chem. Fundam., 15 (1976) 59.
12 P. Proust and J.H. Vera, Can. J. Chem. Eng., 67 (1989) 170.
13 M.J. Huron and J. Vidal, Fluid Phase Equilib., 3 (1979) 255.
14 H. Renon and J.M. Prausnitz, AIChE J., 14 (1968) 135.
15 J.A. Nelder and R. Mead, Comput. J., 7 (1965) 308.

16 T.A. McFall, M.E. Post, S.G. Collins, J.J. Christensen and R.M. Izatt, J. Chem. Thermodyn., 13 (1981) 41.
17 T.A. McFall, M.E. Post, J.J. Christensen and R.M. Izatt, J. Chem. Thermodyn., 14 (1982) 509.
18 J.B. Ott, G.V. Cornett, C.E. Stouffer, B.F. Woodfield, C. Guanquan and J.J. Christensen, J. Chem. Thermodyn., 18 (1986) 867.
19 J.B. Ott, C.E. Stouffer, G.V. Cornett, B.F. Woodfield, C. Guanquan and J.J. Christensen, J. Chem. Thermodyn., 19 (1987) 337.
20 J.B. Ott, J.E. Purdy, B.J. Neely and R.A. Harris, J. Chem. Thermodyn., 20 (1988) 1079.
21 J.J. Christensen, S.P. Christensen, R.S. Schofield, P.W. Faux, P.R. Harding and R.M. Izatt, J. Chem. Thermodyn., 15 (1983) 1151.
22 J.J. Christensen, D.M. Zebolsky, R.S. Schofield, D.R. Cordray and R.M. Izatt, J. Chem. Thermodyn., 16 (1984) 905.
23 J.T. Sipowska, R.C. Graham, B.J. Neely, J.B. Ott and R.M. Izatt, J. Chem. Thermodyn., 21 (1989) 1085.
24 C.J. Wormald, K.L. Lewis and S. Mosedale, J. Chem. Thermodyn., 9 (1977) 27.
25 A.O. Barry, S.C. Kaliaguine and R.S. Ramalho, J. Chem. Eng. Data, 27 (1982) 258.